



Mitogenome of a new *Ramazzottius* species (Tardigrada: Eutardigrada: Ramazzottiidae) discovered in rock pools along with its temperature and desiccation-related proteins repertoire

Matteo Vecchi¹ · Daniel Stec¹

Received: 6 August 2024 / Accepted: 9 October 2024 / Published online: 31 October 2024
© The Author(s) 2024

Abstract

Ramazzottius is a widespread genus of tardigrades with extreme cryptobiotic capabilities. Thanks to its ability to survive desiccation and freezing, this genus is usually recorded from harsh habitats such as exposed mosses and lichens and rock pools. In the last years, research focused on both describing *Ramazzottius* diversity and revealing the molecular mechanisms behind their cryptobiotic capabilities. Despite the research efforts in these fields, much still remains to be discovered. Here we describe a new *Ramazzottius* species from an Italian rock pool by means of integrative taxonomy (morphology, morphometry, and DNA sequencing) and sequenced its genome with Nanopore technology to provide an assembled mitogenome and annotate its Temperature and Desiccation Resistance Proteins (TDPR) repertoire. The new gonochoric species is phylogenetically close to the parthenogenetic *R. varieornatus*, a strain of which (YOKOZUNA-1) has been adopted as model organism for the study of cryptobiosis. The mitogenome of the new species shows perfect synteny with *R. varieornatus* and shares with it most of the TDPR genes. The relative genetic similarity of the new species to the model *R. varieornatus*, combined with unique biological traits (for example the difference in reproductive mode and the unique habitat it colonizes), makes the new species a potential new addition to the range of model tardigrade species.

Keywords *Ramazzottius* · Anhydrobiosis · Nanopore · New species · Mitogenome

Introduction

Tardigrades (also known as water bears) are a group of microscopic animals forming a phylum included in the clade Panarthropoda (Schill, 2018). These meiofaunal animals live in a wide variety of habitats: from aquatic to terrestrial environments, from seas to mountains (Nelson et al., 2018), where they can be found in different substrates such as sediments, soil, bryophytes, lichens, and even in cryoconite holes on glaciers (Nelson et al., 2018; Zawierucha et al., 2016). Thanks to their ability to enter into ametabolic life stages (cryptobiosis), some tardigrades can survive extreme conditions like desiccation and freezing (Hengherr

& Schill, 2018; Rebecchi et al., 2007; Schill & Hengherr, 2018; Zawierucha et al., 2023).

Ramazzottius (Binda & Pilato, 1986) is a genus of limnoterrestrial tardigrades characterized by the presence of apophyses for the insertion of the stylet muscles (AISM) in the shape of blunt hooks, articulated external claws, and sometimes paired elliptical organs on the head. Representatives of *Ramazzottius* are considered xerophilic, often found in habitats exposed to sunlight, often dwelling in bryophytes and lichens (Bartels et al., 2011; Biserov, 1997; Guidetti et al., 2022), but surprisingly also in more aquatic habitats like rock pools sediment (Vecchi et al., 2022). The genus *Ramazzottius* includes different species complexes with generally unresolved phylogenetic relationships among and inside them (Dey et al., 2024; Kihm et al., 2023). The most common and widespread group is the polyphyletic *oberhaeuseri* morpho-group, characterized by eggs with hemispherical processes and rampant cryptic and pseudocryptic speciation (Guidetti et al., 2022; Stec et al., 2018). The monophyletic *baumanni* and *szeptyckii* complexes from the tropics are characterized by peculiar ornamented cuticle and

✉ Matteo Vecchi
matteo.vecchi15@gmail.com; m.vecchi@isez.pan.krakow.pl

¹ Institute of Systematics and Evolution of Animals, Polish Academy of Sciences, Sławkowska 17, 31-016, Kraków, Poland

their eggs are unknown (Dey et al., 2024). *Cryoconicus*, recently separated from *Ramazzottius* and characterized by peculiar AISM and claws morphology and by an intense body pigmentation (Guidetti et al., 2019; Zawierucha et al., 2018), has been suggested to not be valid (Dey et al., 2024), and thus be part of *Ramazzottius*. Additionally, species that do not fall into any of these groups are present and are generally characterized by body with relatively plain sculpture (compared to the *baumanni* and *szeptyckii* complexes) and with egg processes usually in the shape of spines and cones (Bertolani & Kinchin, 1993; Biserov, 1997; Guidetti et al., 2019; Kihm et al., 2023; Stec et al., 2016).

The genus *Ramazzottius* made its way into becoming a model taxon for the study of extreme resistance mechanisms in tardigrades and their biological interactions (see for example Emdee et al., 2024; Horikawa, 2008; Horikawa et al., 2008, 2013); however, at this time, experimental and genomic data are available for only one species of the genus (*R. varieornatus* Bertolani & Kinchin, 1993 strain YOKO-ZUNA-1; Horikawa et al., 2008), precluding a comparative approach across related species.

Tardigrades from rock pools have been investigated thoroughly only recently (Vecchi et al., 2022); however, two new species from these habitats have been discovered and already described (Vecchi et al., 2023a, 2023b) showing their potential as source of tardigrades biodiversity. *Ramazzottius* from rock pools have been shown to possess an incredible tolerance to freeze–thaw cycles (Zawierucha et al., 2023), even higher than tardigrades taxa adapted to life on glaciers, highlighting the extreme adaptations encountered in tardigrades from this habitat.

Ramazzottius claudii sp. nov. from a rock pool in the Italian Apennines is described here by means of integrative taxonomy using light microscopy (LM), scanning electron microscopy (SEM), and DNA sequencing. To provide the community with more genomic data to help unravel the resistance mechanisms of tardigrades, we also provide for the first time in a tardigrade species description, its annotated whole mitochondrial genome and its repertoire of Temperature and Desiccation-Related Proteins (Fleming et al., 2024) sequenced with long-read third generation sequencing technology (Nanopore).

Materials and methods

Sampling and tardigrades extraction

A rock pool sediment sample was collected on 27/06/2020 in Corniglio, Parma, Italy (44.3960680 10.00437) by scraping the sediment with a clean plastic spoon into a plastic tube. The sample was kept desiccated and frozen at -20°C until processing. The sample was processed to extract tardigrades

as in (Vecchi et al., 2023a). The sample was collected under sampling permit N.0001671/2020 from Parco Nazionale Appennino Tosco-Emiliano (Italy).

Additional material

Individuals of *Hebesuncus conjungens* (Thulin, 1911) were extracted from a moss collected on 15/06/2023 in Corniglio, Parma, Italy (44.3800370 10.0414130) for DNA sequencing (Sample collected under sampling permit N.0003526/2021 from Parco Nazionale Appennino Tosco-Emiliano, Italy). Previously extracted *Ramazzottius* individuals (S66.01 and S132.02 from Vecchi et al., 2022), and already sequenced for COI, were used for sequencing additional markers (18S, 28S and ITS2).

Microscopy and imaging

Specimens for light microscopy were mounted on microscope slides in a small drop of Hoyer's medium, secured with a cover slip and dried at 50°C for a week. Slides were examined under a Leica DMLB light microscope with phase contrast (PCM), associated with a digital camera. For structures that could not be satisfactorily focused on a single light microscope photograph, a stack of 2–5 images were taken with an equidistance of ca. $0.2\text{ }\mu\text{m}$ and assembled manually into a single deep-focus image in GIMP v.2–10 (GIMP Development Team, 2019). Specimens for scanning electron microscopy were prepared according to the protocol of (Camarda et al., 2023). Specimens were examined under high vacuum in a Versa 3D Dual Beam Scanning Electron Microscope at the ATOMIN facility of the Jagellonian University, Kraków, Poland. For structures that could not be satisfactorily focused in a single photograph, a stack of 2–6 images were taken with an equidistance of ca. $0.2\text{ }\mu\text{m}$ and assembled manually into a single deep-focus image. All figures were assembled in Figure J (Mutterer & Zinck, 2013).

Morphometrics and morphological nomenclature

All measurements are given in micrometers (μm). Structures were measured only if their orientation was suitable. Body length was measured from the anterior extremity to the posterior end of the body, excluding the hind legs. Buccal tube length and the level of the stylet support insertion point were measured according to (Pilato, 1981). The *pt* index is the ratio of the length of a given structure to the length of the buccal tube (Pilato, 1981). Claws were measured according to (Stec et al., 2018) and ratios are provided according to (Vecchi et al., 2023b). Morphometric data were handled using the “Parachela” ver. 1.7 template available from the Tardigrada Register (Michalczyk & Kaczmarek, 2013).

The raw morphometric data are provided as Supplementary Materials (Online resources 01).

Genotyping

DNA was extracted from individual animals following a Chelex® 100 resin (BioRad) extraction method by Casquet et al. (2012) with modifications described in detail in Stec et al. (2020). Briefly, animals were individually placed in 40 µl of a 4% Chelex® solution with the addition of 3 µl of proteinase K (20 mg/ml, activity ≥ 30 U/mg) and incubated in a thermomixer at 56 °C and 750 rpm for 30 min. The solution was then heated at 70 °C for 10 min and the supernatant was transferred to a new microcentrifuge tube and used as input for PCR. We sequenced four DNA fragments, three nuclear (18S rRNA, 28S rRNA, and ITS2) and one mitochondrial (COI). All fragments were amplified and sequenced according to the primers and protocols described in Stec et al. (2020). Sequencing products were read with the ABI 3130xl sequencer at the Genomed company (Warsaw, Poland).

Phylogenetic reconstruction

A phylogenetic reconstruction was made using the concatenated markers 18S rRNA + 28S rRNA + COI + ITS2 from *Ramazzottius* clade A (sensu Dey et al., 2024), with the addition of sequences from *Ramazzottius kretschmanni* Guidetti et al., 2022, *Ramazzottius groenlandensis* Kihm et al., 2023 and the sequences newly generated for this study. Sequences of *H. conjugens* were used as outgroup. The GenBank accession numbers of the sequences and those used in the phylogenetic reconstruction are presented in Table 1.

The 18S rRNA, 28S rRNA, and ITS2 sequences were aligned with MAFFT ver. 7 (Katoh, 2002; Katoh & Toh, 2008) with the G-INS-i method (thread=4, threadtb=5, threadit=0, reorder, adjustdirection, anysymbol, maxiterate=1000, retree 1, globalpair input). The COI sequences were aligned according to their amino acid sequences (translated using the invertebrate mitochondrial code) with the MUSCLE algorithm (Edgar, 2004) in MEGA7 with default settings (all gap penalties=0, max iterations=8, clustering method=UPGMB, lambda=24). Alignments were visually inspected and trimmed in MEGA7. Sequences were concatenated with the R package “concatipede” v1.0.0 (Vecchi & Bruneaux, 2021).

Model selection and maximum likelihood (ML) phylogenetic reconstruction were performed with IQTREE (Trifinopoulos et al., 2016) on the partitioned dataset on the IQTREE web server (<http://iqtree.cibiv.univie.ac.at/>) with default parameters and ultrafast bootstrap with 1000 replicates. The concatenated alignment is available as Supplementary Materials (DATA block of Online resources 02).

Model selection results are available as Supplementary Material (Online resources 03).

For Bayesian Inference (BI) phylogenetic reconstruction, model selection was performed for each alignment partition (6 in total: 18S rRNA, 28S rRNA, ITS-2 and three COI codons) using PartitionFinder2 (Lanfear et al., 2016). Bayesian inference (BI) phylogenetic reconstruction was performed using MrBayes v3.2.6 (Ronquist et al., 2012). Two runs (one cold chain and three heated chains each) of 20 million generations were used with a burn-in of 2 million generations, sampling a tree every 1000 generations. Posterior distribution sanity was checked using Tracer v1.7 (Rambaut et al., 2018). The MrBayes input file with the input alignment is available as Supplementary Materials (Online resources 02); model selection results are available as Supplementary Material (Online resources 03). Both the IQTREE tree and the MrBayes consensus tree are available as Supplementary Materials (Online resources 04). The phylogenetic trees were visualized with FigTree (Rambaut, 2007) and edited with Inkscape (Inkscape Project, 2020).

Whole-genome amplification and sequencing

One individual *Ramazzottius* of the new species (Ram_IT.158_WGA_1) was starved in sterile distilled water for 24 h at 18°C and then washed twice in sterile distilled water. The individual was then dissected in a 0.5-µl drop of sterile distilled water with a sterilized entomological needle and used as starting material for a whole-genomic amplification (WGA) reaction using the REPLI-g Mini Kit (Cat. No. 150023, Qiagen) according to the manufacturer protocol. The reaction product was purified with a GeneMAGNET PCR/DNA Clean-Up Purification Kit (Cat. No. E3420, EURx) and the dsDNA was quantified using a Qubit Fluorometric assay. Approximately 2 µg of amplified DNA were debranched for 1 h with T7 Endonuclease I (Cat. No. M0302, New England Biolabs) according to the manufacturer protocol. The reaction product was again purified with GeneMAGNET and quantified with Qubit. The dsDNA was used as input for library preparation with the Oxford Nanopore Native Barcoding Kit 24v14 (Cat. No. SQK-NBD114.24, Oxford Nanopore Technologies—ONT) following the ONT community protocol NBE_9169_V114_REVP_15SEP2022 and sequenced on part of a FLO-MIN114 R10 flow cell using a MinION Mk1B for 48 h. Basecalling, demultiplexing, and adaptors trimming were done with the software MinKNOW (ONT) using a fast basecalling strategy. Sequences of the DNA control sample (DCS) introduced during library preparation were removed with *chopper* (De Coster & Rademakers, 2023). The raw reads were submitted to NCBI SRA (BioProject PRJNA1082523, accession number SRR28173874).

Table 1 GenBank accession numbers of the sequences used in the phylogenetic reconstruction

	SSU (18S)	LSU (28S)	COI	ITS2	Source
<i>Ramazzottius claudii</i> n.sp. IT.158.1	PQ108467	PQ108476	PQ109084	PQ110585	This study
<i>Ramazzottius claudii</i> n.sp. IT.158.3	PQ108468	PQ108477	PQ109085	PQ110586	This study
<i>Ramazzottius claudii</i> n.sp. S62 1			MW306836		Vecchi et al. (2022)
<i>Ramazzottius claudii</i> n.sp. S62 2			MW306835		Vecchi et al. (2022)
<i>Ramazzottius claudii</i> n.sp. S66 1	PQ108470	PQ108475	MW306833	PQ110584	This study; Vecchi et al. (2022)
<i>Ramazzottius claudii</i> n.sp. S66 2			MW306834		Vecchi et al. (2022)
<i>Ramazzottius claudii</i> n.sp. S67 1			MW306832		Vecchi et al. (2022)
<i>Ramazzottius</i> AT.002 b			MG432811	MG432814	Stec et al. (2018)
<i>Ramazzottius</i> DE.002 a			MG573257		Stec et al. (2018)
<i>Ramazzottius</i> DE.002 b		MG432817	MG432812	MG432815	Zawierucha et al. (2018)
<i>Ramazzottius groenlandensis</i> 1	OR600266	OR600265	OR596527		Kihm et al. (2023)
<i>Ramazzottius groenlandensis</i> 2			MG432810		Zawierucha et al. (2018)
<i>Ramazzottius groenlandensis</i> 3			EU251381		Faurby et al. (2008)
<i>Ramazzottius groenlandensis</i> 4			EU251382		Faurby et al. (2008)
<i>Ramazzottius kretschmanni</i> T1			OM370801	OM402517	Guidetti et al. (2022)
<i>Ramazzottius kretschmanni</i> T2			OM370802	OM402518	Guidetti et al. (2022)
<i>Ramazzottius kretschmanni</i> T3			OM370803	OM402519	Guidetti et al. (2022)
<i>Ramazzottius kretschmanni</i> T4			OM370804	OM402520	Guidetti et al. (2022)
<i>Ramazzottius oberhaeuseri</i> FR.12	MG573241	MG573242	MG573244	MG573243	Stec et al. (2018)
<i>Ramazzottius</i> PL.023			MG573253		Stec et al. (2018)
<i>Ramazzottius</i> PL.140 1			MG573248		Stec et al. (2018)
<i>Ramazzottius</i> PL.140 2			MG573249		Stec et al. (2018)
<i>Ramazzottius</i> PL.141			MG573247		Stec et al. (2018)
<i>Ramazzottius</i> PT.010 1			MG573245		Stec et al. (2018)
<i>Ramazzottius</i> PT.010 2			MG573246		Stec et al. (2018)
<i>Ramazzottius</i> Rama1			EU251380		Faurby et al. (2008)
<i>Ramazzottius</i> Rama2			EU251379		Faurby et al. (2008)
<i>Ramazzottius</i> Ro-Nivaa-1			EF620418	EF620419	Møbjerg et al. (2007)
<i>Ramazzottius</i> S132 1	PQ108469	PQ108474	MW306838	PQ110583	This study; Vecchi et al. (2022)
<i>Ramazzottius</i> S132 2			MW306837		Vecchi et al. (2022)
<i>Ramazzottius</i> S49 1			MW306839		Vecchi et al. (2022)
<i>Ramazzottius</i> S49 2			MW306840		Vecchi et al. (2022)
<i>Ramazzottius</i> S67 2			MW306841		Vecchi et al. (2022)
<i>Ramazzottius subanomalous</i> 1	MF001997	MF001998	MF001999	MG432819	Stec et al. (2017)
<i>Ramazzottius subanomalous</i> 2			KU900021	KU900019	Stec et al. (2016)
<i>Ramazzottius</i> Tar398	FJ435728		FJ435799		Guil and Giribet (2012)
<i>Ramazzottius</i> Tar400	FJ435727		FJ435800		Guil and Giribet (2012)
<i>Ramazzottius varieornatus</i> YOKOZUNA-1		MG432818	MG432813	MG432816	Zawierucha et al. (2018)
<i>Hebesuncus conjugens</i> IT.148.2	PQ108465	PQ108478	PQ109086	PQ110587	This study
<i>Hebesuncus conjugens</i> IT.148.3	PQ108466	PQ108479	PQ109087	PQ110588	This study

Mitogenome assembly and annotation

The clean reads were blasted against a tardigrades mitochondrial proteins database (compiled from tardigrade mitochondrial protein sequences present in GenBank; Online resources 05) using DIAMOND (Buchfink et al., 2015; options: –sensitive –max-target-seqs 1) and the matching query sequences were extracted with *seqtk* (<https://github.com/lh3/seqtk>) and assembled with Flye v 2.9.3 (Kolmogorov et al., 2019; Lin et al., 2016) with 5 polishing round (options: -i 5). The assembled sequences were visualized with Bandage (Wick et al., 2015) and the identity of the mitogenome contig confirmed by blastn against the *Ramazzottius varieornatus* YOKOZUNA-1 mitogenome (GenBank NC_031407). A final polishing of the retrieved mitogenome contig was done with medaka v 1.11.3 (<https://github.com/lh3/seqtk>)

and assembled with Flye v 2.9.3 (Kolmogorov et al., 2019; Lin et al., 2016) with 5 polishing round (options: -i 5). The assembled sequences were visualized with Bandage (Wick et al., 2015) and the identity of the mitogenome contig confirmed by blastn against the *Ramazzottius varieornatus* YOKOZUNA-1 mitogenome (GenBank NC_031407). A final polishing of the retrieved mitogenome contig was done with medaka v 1.11.3 (<https://github.com/lh3/seqtk>)

[com/nanoporetech/medaka](https://nanoporetech/medaka)) using all the original reads. The mitochondrial genome was annotated with MITOS2 (Bernt et al., 2013; Donath et al., 2019) on the Galaxy Europe web server (<https://usegalaxy.eu/>). The annotation was inspected and curated by hand and a GenBank flat file was produced using the scripts `mitos2fasta.py` and `aln2tbl.py` (<https://github.com/IMEDEA/mitogenomics>), and `table2asn` (https://ftp.ncbi.nlm.nih.gov/asnl-converters/by_program/). The mitogenome was visualized with OGDRAW (Greiner et al., 2019). Coverage data was extracted from the medaka BAM files using the R package “`gmoviz`” (Zeglinski et al., 2021). Divergence and synteny of the mitochondrial genomes of the new species and *R. varieornatus* YOKOZUNA-1 (NC_031407) were visualized using the R packages “`ggplot2`” (Wickham, 2016), “`genoPlotR`” (Guy et al., 2010), “`gggenes`” (Wilkins, 2024), and “`patchwork`” (Pedersen, 2023). The newly assembled mitogenome sequence is available in GenBank (Accession number PP419898).

Temperature and desiccation-related protein genes annotation

Genes in the new *Ramazzottius* species were identified from a genome assembly of all clean reads obtained with Flye and Medaka as explained above. The completeness of the assembly was evaluated with BUSCO (Simão et al., 2015) (lineage metazoa_odb10) on the gVolante webserver (Nishimura et al., 2017). Contigs containing potential Temperature and Desiccation-Related Proteins (TDRPs) sequences were extracted with DIAMOND (options: `-sensitive`) using the eutardigrade TDRPs (CAHS, MAHS, MRE11, SAHS) sequences provided by Fleming et al. (2024), with the addition of Dsup (GenBank LC050827). The identified contigs were annotated ab initio on the AUGUSTUS webserver (Hoff & Stanke, 2013; Stanke et al., 2008) trained on the

genome and proteome of *R. varieornatus* YOKOZUNA-1 (<http://kumamushi.org/>). TDRPs were identified among the predicted proteins with BLASTp (e-value = $10e-10$) against the TDRPs protein sequences from Fleming et al., (2024). The identified protein sequences (and their relative coding sequences) were manually curated to confirm their identity. Maximum Likelihood phylogenies of the main TDRPs groups were obtained as in Fleming et al. (2024), with the addition of the sequences produced in this study.

Results

Phylogenetic reconstruction

The phylogenetic reconstruction was performed with both Bayesian inference (BI) and maximum likelihood (ML) methods with the models provided in Online Resources 03. Both methods retrieved congruent topologies, even though ML provided a generally less resolved tree (Fig. 1; Online Resource 03). In both reconstruction topologies, the new *Ramazzottius* species was found in a clade (pp = 1, BS = 98%) with *R. varieornatus* YOKOZUNA-1 and *Ramazzottius* aff. *varieornatus* from Italy.

Genome sequencing and assembly

The sequencing run resulted in 3.69 Gb of sequences. The summary statistics of the raw reads are presented in Table 2. The assembly metrics and the BUSCO score were compared to those of the *R. varieornatus* YOKOZUNA-1 assembly generated by Hashimoto et al. (2016) (available at <http://www.kumamushi.org/data/YOKOZUNA-1.scaffolds.fa>). The assembly has a comparable size to *R. varieornatus* YOKOZUNA-1 (Table 2), but it is more fragmented. The

Table 2 Raw reads and assembly metrics

	<i>R. claudii</i> sp. nov.. raw reads	<i>R. claudii</i> sp. nov. assembly	<i>R. varieornatus</i> YOKOZUNA-1 assembly
Size	3.69 Gb	62.89 Mb	55.82 Mb
N of sequences	4,817,658	1468	199
N of sequences > 1 kb	738,949	1415	198
N of sequences > 10 kb	28,279	800	36
GC content (%)	47.4	47.8	47.2
N50	1399	157,755	4,740,345
L50	485,725	109	4
N90	280	18,551	1,295,620
L90	3,074,768	549	15
BUSCO		C: 71.6% [S: 69.4%, D: 2.2%] F: 7.4% M: 21.0% n: 954	C: 74.4% [S: 73.2%, D: 1.2%] F: 7.0% M: 18.6% n: 954

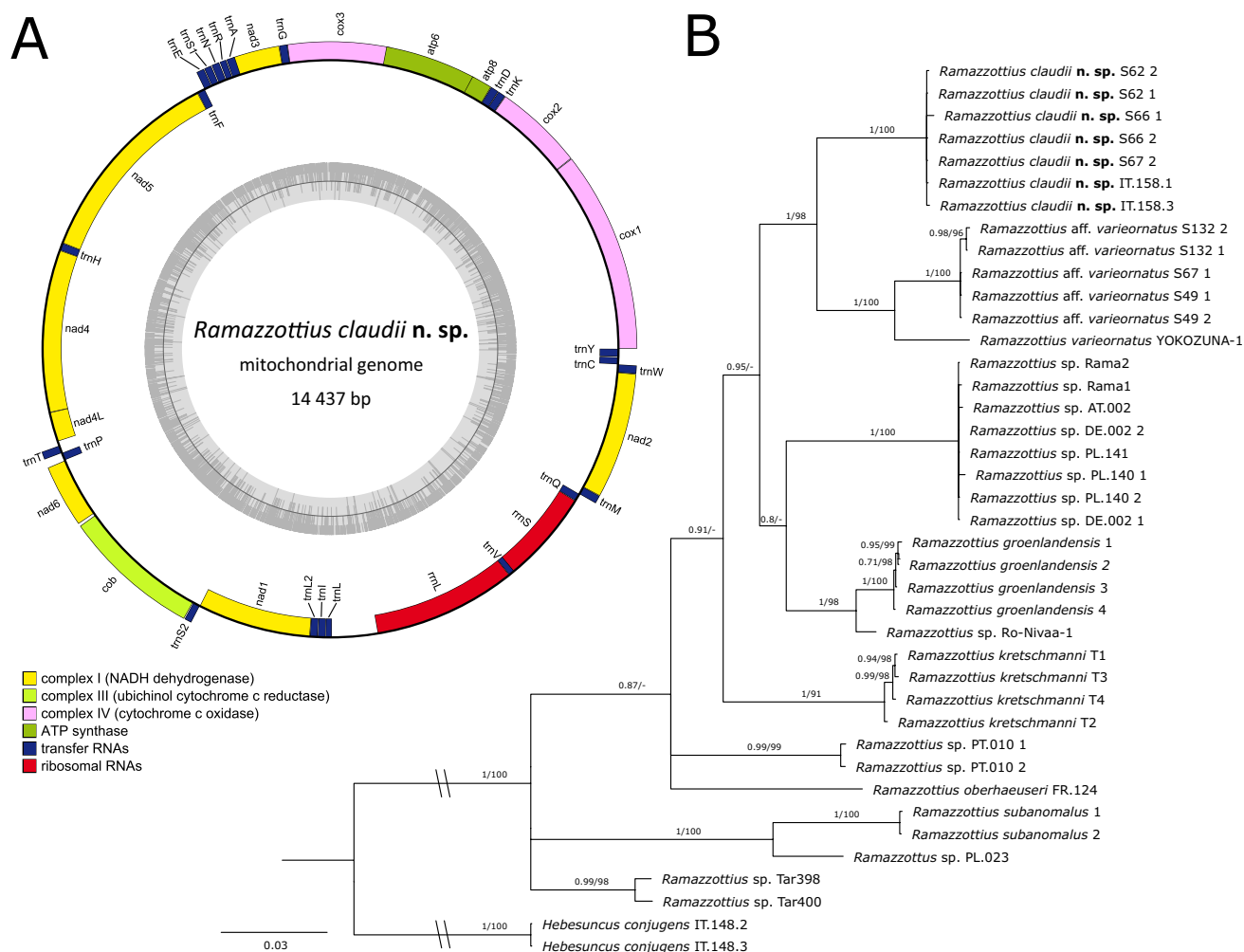


Fig. 1 *Ramazzottius claudii* sp. nov. mitogenome and phylogenetic position. **A** Mitogenome visualization: inner circle represents GC content. Direction of transcription is clockwise for genes in on the inner side, whereas it is anticlockwise for the genes on the external side. **B** Topology of the Bayesian Inference (BI) phylogenetic recon-

struction of *Ramazzottius* clade A (sensu Dey et al., 2024): values above branches represent BI posterior probabilities/ML bootstrap (“-” indicated bootstrap value < 70% or node not present in ML phylogenetic reconstruction), scale bar indicates substitutions/site

BUSCO score of the new assembly (71.6%) is comparable to the one of *R. varieornatus* YOKOZUNA-1 (74.4%). The assembly of *R. claudii* sp. nov. genome generated in this study can be found at <https://doi.org/https://doi.org/10.6084/m9.figshare.27061267>.

Mitogenome sequencing

Of all the raw reads, about 1.75% were of mitochondrial origin. The mitogenome assembly is 14,437 bp in length (Fig. 1) with an average coverage of 4486× (min 1506×–max 6785×). Two ribosomal RNAs (rrnS and rrnL), 22 tRNAs (with two trnL and trnS), 2 ATP synthase genes, and the genes for the complexes I, III, and IV are present. A putative unannotated control region is present between

rrnL and trnL. The order of the genes is identical to the mitogenome of *Ramazzottius varieornatus* YOKOZUNA-1 (Fig. 2), with an average nucleotidic divergence of 20.6%.

TDRP identification

CAHS

A total of 15 CAHS genes were identified (Table 3, Online resources 06). The phylogenetic reconstructions based of the CAHS protein sequences are similar to the ones found by (Fleming et al., 2024), with the exceptions of the CAHS families 2, 3, and 5 which have been found paraphyletic (Online resources 06).

Fig. 2 Divergence and synteny of *Ramazzottius claudii* sp. nov. and *R. varieornatus* YOKOZUNA mitogenomes. In black: nucleotide divergence; in red: indel divergence. Divergence was calculated on 250 bp sliding windows; Arrow directions indicate transcription direction

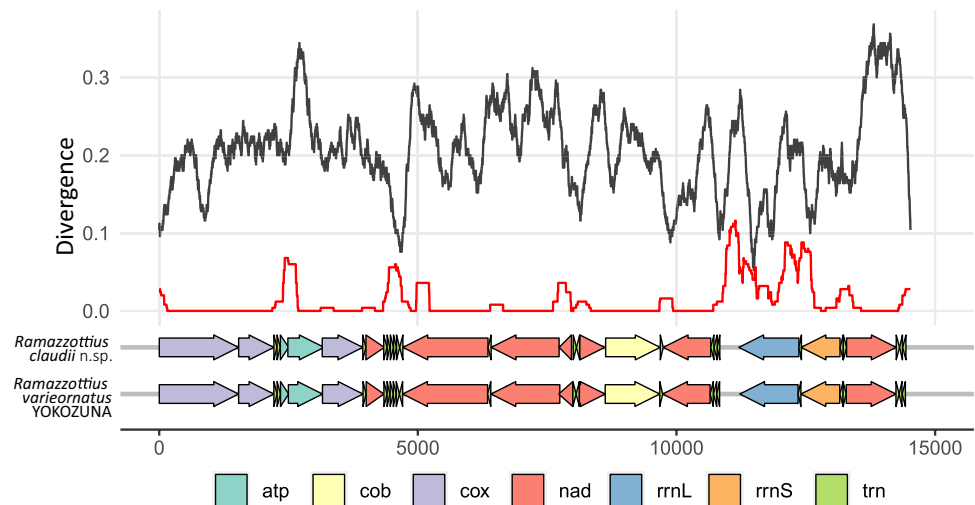


Table 3 GenBank accession numbers of the TDRPs genes identified in *Ramazzottius claudii* sp. nov. classified according to their homology with the ones from *R. varieornatus* YOKOZUNA-1

Gene in <i>R. varieornatus</i> YOKOZUNA-1	<i>R. claudii</i> sp. nov.	Gene in <i>R. varieornatus</i> YOKOZUNA-1	<i>R. claudii</i> sp. nov.	Gene in <i>R. varieornatus</i> YOKOZUNA-1	<i>R. claudii</i> sp. nov.
CAHS		SAHS Subfamily 1		MAHS	
CAHS 1a	PQ117601	SAHS 2	PQ117620	MAHS 1	PQ117614
CAHS 1b	PQ117608	SAHS 7	PQ117618	MRE11	
CAHS 2a	PQ117603	SAHS 12		MRE11 A	PQ117615
CAHS 3a	PQ117609	SAHS 8	PQ117619	MRE11 B	
CAHS 3b	PQ117599	SAHS 9	Not found	MRE11 C	
CAHS 3c	PQ117607	SAHS 10	Not found	MRE11 D	
CAHS 4a	PQ117602	SAHS 11	PQ117615	FABP	
CAHS 5a	PQ117610	SAHS Subfamily 2		FABP 1	Not found
CAHS 5b	PQ117604	SAHS 1	PQ117617	FABP 2	PQ117628
CAHS 5c	PQ117606	SAHS 3	PQ117621	FABP 3	PQ117625
CAHS 6a	PQ117612	SAHS 4	PQ117616	FABP 4	PQ117627
CAHS 6b	PQ117613	SAHS 5	PQ117623	FABP 5	PQ117626
CAHS 6c	Not found	SAHS 6	PQ117622	FABP 6	PQ117624
CAHS 6d	PQ117611	SAHS 13	Not found	FABP 7	Not found
CAHS 7a	PQ117605	Dsup			
		Dsup	PQ356341		

SAHS–FABP

A total of 8 SAHS genes were identified (Table 3, Online resources 07). The Macrobiotidae SAHS and the SAHS subfamily 1 were recovered as monophyletic (Online resources 07), while SAHS subfamily 2 was recovered as paraphyletic. 5 FABP (fatty acid binding proteins, see (Fleming et al., 2024) for their phylogenetic relation with SAHS) genes were also recovered and included in the phylogeny.

MAHS

A single MAHS gene was found (Table 3, Online resources 09).

MRE11

A single MRE11 gene was identified (Table 3, Online resources 09).

Dsup

A single Dsup gene was identified (Table 3, Online resources 10).

Taxonomic account

Ramazottius claudii sp. nov. Vecchi & Stec, 2024

Zoobank registration: urn:lsid:zoobank.org:act:0B3D4075-0C0B-4552-B7B6-73EC10711ED4

Ramazottius sp. A in (Vecchi et al., 2022)

Ramazottius sp. Italy in (Zawierucha et al., 2023)

Type locality. Rock pool sediment from vicinity of Sella del Marmagna, Corniglio, Parma, Italy (44°23'45.8"N 10°00'15.7"E).

Material examined. Holotype (Slide IT.158.7), 23 paratypes (Slides IT.158.4 – IT.158.10) and 20 eggs (Slides IT.158.01 – IT.158.03) mounted on slides in Hoyer's medium. 4 animals (Stub TAR.2.06) and 5 eggs (Stub TAR.2.07) mounted on stubs for SEM. 3 animals used for DNA sequencing (Ram.sp.IT.158.01, Ram.sp.IT.158.03 and Ram_IT.158_WGA_1).

Material repository. Tardigrada collection of the Institute of Systematics and Evolution of Animals (Polish Academy of Sciences), Sławkowska 17, 31–016, Kraków, Poland.

Etymology. This species is dedicated to Claudio Ferrari (University of Parma, Italy), to acknowledge his constant support and help in exploring the Italian Northern Apennines in search of rock pools.

(Tables 4 and 5, Figs. 3, 4, 5, 6, 7, 8, and 9, Online resources 01).

Description. *Animals* (morphometrics in Table 4, raw measurements in Online resources 01): Eyes absent in live individuals. Pigmentation of the cuticle red-brown, distributed in one ring around the mouth, a dorso-caudal continuous band, and 8 lateral-ventral bands (Fig. 3). Cuticle with faint sculpture, more visible in the dorso-caudal part of the body (Figs. 4 and 5). A pair of sensory organs present on the head (Fig. 5A). The sculpture is composed by rounded polygonal granules; however, in some individuals (in particular in the caudal portion of bigger individuals), the granules have an elongated “spindle” shape (Figs. 4 and 5).

Bucco-pharyngeal apparatus of the *Ramazottius*-type (Fig. 6). Mouth opening antero-ventral. Oral cavity armature visible under PCM (Fig. 6B and C). The armature is composed of one band of teeth, located in the posterior oral cavity (Fig. 6B and C). The band composed of a single row of large

and regularly spaced granular teeth. In ventral view, the teeth are less visible and seem connected to the posterior edge of the oral cavity (Fig. 6C). Under PCM, other structures within oral cavity not visible (Fig. 6B and C). Apophyses for the insertion of stylet muscles (AISM) in the shape of blunt hooks and asymmetrical in size and shape with respect to the frontal plane (Fig. 6D). Stylet furcae with rounded ends. Buccal tube with a posterior bend and thickened walls posteriorly from the stylet support insertion point. Pharyngeal bulb (bulbus) almost oval, with apophyses and two clearly separated macroplacoids. Pharyngeal apophyses triangular, smaller than macroplacoids (Fig. 6E). Macroplacoid length configuration $2 < 1$. Microplacoid and septulum absent (Fig. 6E). Macroplacoids are usually roundish; however, in bigger specimens, they look slightly more elongated. Constrictions in the macroplacoids are present. In the first macroplacoid a central constriction is present, whereas in the second macroplacoids a constriction in central-posterior position is present.

Claws of the *Ramazottius*-type. Primary branches of external and posterior claws long and thin. A non-sclerotized light refracting unit (LRU) is present between the claw base and the primary branch, which are connected by a couple of thin cuticular filaments (Fig. 7A, B).

Internal and anterior claws much smaller and of a different shape than external claws (Fig. 7). Claws with smooth pseudolunules (Fig. 7B). Accessory points on primary branches of all claws present (Fig. 7D–E). Bars and other cuticular thickenings on legs, absent. A papilla is present on the external side of legs IV, but not always visible depending on the animal positioning (Fig. 7C).

Eggs (morphometrics in Table 5, raw measurements in Online resources 01): Laid freely, white and spherical, covered in processes with shape ranging from spike-like to filamentous (Fig. 8). The processes exhibit extreme diversity in size, with most of them being within the range of 4.6–14.4 μm , but with some of them reaching up to 27.9 μm (Fig. 8C). Egg processes and surface between processes dotted under PCM, smooth under SEM (Fig. 8I).

Males Individuals with gonad filled with developing spermatids were found, indicating the presence of males (Fig. 9).

DNA sequences.

SSU (18S): PQ108467 – 8, PQ108470;

LSU (28S): PQ108475 – PQ108477;

COI: MW306832 – MW306836, PQ109084 – 5;

ITS-2: PQ110584 – 6.

Differential diagnosis

By having eggs with dotted chorion and elongated processes, *R. claudii* sp. nov. is similar to six other species, however it differs from:

Table 4 Summary of animals morphometrics of *Ramazzottius claudii* sp. nov. *cbt* and *pr* ratios according to Vecchi et al. (2023b)

Character	N	Range						Mean		SD		Holotype	
		μm			<i>pt</i>			μm	<i>pt</i>	μm	<i>pt</i>	μm	<i>pt</i>
Body length	20	292	–	488	934	–	1205	391	1061	55	67	379	1120
Buccal tube													
Buccal tube length	20	29.7	–	43.9	–	–	–	36.7	–	3.9	–	33.8	–
Stylet support insertion point	20	19.9	–	30.0	65.9	–	70.4	25.0	68.1	2.8	1.3	22.9	67.8
Buccal tube external width	20	2.5	–	3.6	7.1	–	9.8	3.0	8.3	0.3	0.6	3.3	9.8
Buccal tube internal width	18	1.0	–	2.0	3.0	–	6.0	1.4	3.9	0.2	0.7	2.0	6.0
Placoid lengths													
Macroplacoid 1	19	3.7	–	6.7	11.2	–	16.6	4.9	13.2	0.9	1.5	3.8	11.3
Macroplacoid 2	19	3.0	–	5.9	9.6	–	14.6	4.3	11.5	0.8	1.2	3.6	10.7
Macroplacoid row	19	7.0	–	12.9	22.9	–	32.0	9.9	26.6	1.8	2.5	8.2	24.3
Claw 1 lengths													
External base	19	8.0	–	13.1	22.9	–	32.2	10.0	27.6	1.3	2.6	9.4	27.7
External primary branch	18	12.5	–	19.1	38.9	–	48.9	16.0	43.9	2.1	2.6	15.1	44.8
External secondary branch	17	6.9	–	11.4	23.4	–	32.6	9.4	26.1	1.3	2.2	9.4	27.7
External <i>cbt</i> ratio	18	49.0	–	73.8	–	–	–	63.1	–	6.0	–	61.9	–
External <i>br</i> ratio	16	49.8	–	67.4	–	–	–	59.1	–	3.9	–	–	–
External total	17	18.8	–	31.0	60.6	–	78.0	24.8	68.5	3.3	5.2	24.3	71.8
Internal base	13	4.5	–	8.5	13.8	–	22.6	7.2	19.6	1.2	2.6	7.5	22.2
Internal primary branch	12	6.7	–	12.5	20.1	–	31.1	9.8	26.7	1.7	3.0	8.8	25.9
Internal secondary branch	13	4.4	–	10.3	13.3	–	25.5	7.5	20.7	1.4	3.2	7.3	21.7
Internal <i>cbt</i> ratio	12	47.0	–	93.4	–	–	–	74.2	–	13.4	–	85.5	–
Internal <i>br</i> ratio	12	63.4	–	93.9	–	–	–	76.9	–	8.4	–	–	–
Internal total	10	10.8	–	16.6	32.4	–	41.0	13.2	36.4	1.7	2.6	?	?
Claw 2 lengths													
External base	19	8.3	–	13.5	24.8	–	35.2	10.8	29.5	1.5	2.6	10.4	30.8
External primary branch	18	11.1	–	21.4	37.2	–	52.8	16.4	45.0	2.3	3.5	16.5	48.7
External secondary branch	19	7.5	–	11.7	24.4	–	30.7	10.0	27.4	1.1	1.8	9.6	28.4
External <i>cbt</i> ratio	18	56.9	–	77.3	–	–	–	65.9	–	7.5	–	63.3	–
External <i>br</i> ratio	18	51.2	–	75.1	–	–	–	61.4	–	5.7	–	–	–
External total	14	22.2	–	33.1	61.8	–	82.3	26.8	73.5	3.5	5.4	25.0	73.8
Internal base	15	3.6	–	9.5	10.3	–	22.2	7.1	19.5	1.4	2.9	7.5	22.2
Internal primary branch	15	7.7	–	14.4	24.0	–	37.7	10.4	28.6	1.7	3.4	8.8	25.9
Internal secondary branch	11	6.1	–	9.8	18.2	–	25.6	8.2	22.7	1.1	2.4	8.7	25.6
Internal <i>cbt</i> ratio	15	42.9	–	85.6	–	–	–	68.6	–	11.7	–	85.6	–
Internal <i>br</i> ratio	11	59.0	–	98.9	–	–	–	80.0	–	12.1	–	–	–
Internal total	14	10.1	–	17.7	29.9	–	44.2	14.0	38.3	2.4	3.6	10.1	29.9
Claw 3 lengths													
External base	19	7.6	–	13.9	25.4	–	34.3	10.8	29.2	1.7	2.3	9.3	27.5
External primary branch	20	13.6	–	20.0	44.3	–	53.2	17.6	47.8	1.9	2.3	17.4	51.6
External secondary branch	18	6.8	–	12.1	22.8	–	29.9	9.8	26.8	1.4	1.8	8.7	25.8
External <i>cbt</i> ratio	19	52.9	–	73.3	–	–	–	61.2	–	5.7	–	53.4	–
External <i>br</i> ratio	18	49.3	–	62.8	–	–	–	56.0	–	4.2	–	–	–
External total	15	20.6	–	34.8	64.7	–	85.8	26.6	72.6	4.2	6.0	25.5	75.5
Internal base	17	5.8	–	11.8	17.6	–	28.2	7.9	21.6	1.3	2.6	6.8	20.2
Internal primary branch	18	7.3	–	12.9	21.2	–	33.6	10.3	28.6	1.8	3.6	9.6	28.4
Internal secondary branch	17	5.9	–	10.9	16.2	–	30.1	8.5	23.3	1.5	3.3	8.3	24.4
Internal <i>cbt</i> ratio	17	59.1	–	106.1	–	–	–	75.8	–	12.9	–	71.1	–
Internal <i>br</i> ratio	17	58.3	–	141.6	–	–	–	82.1	–	18.1	–	–	–
Internal total	15	12.5	–	17.3	35.0	–	43.0	14.5	39.6	1.5	2.6	13.8	40.8

Table 4 (continued)

Character	<i>N</i>	Range						Mean		SD		Holotype	
								μm	<i>pt</i>	μm	<i>pt</i>	μm	<i>pt</i>
Claw 4 lengths													
Anterior base	13	6.3	–	10.0	15.3	–	26.5	8.2	22.2	1.3	3.1	8.5	25.2
Anterior primary branch	13	9.0	–	13.6	26.1	–	35.8	11.4	30.7	1.4	2.9	12.1	35.8
Anterior secondary branch	9	6.2	–	12.8	18.7	–	31.5	9.7	25.9	2.1	4.2	9.5	28.2
Anterior <i>cbt</i> ratio	12	58.8	–	82.5		–		71.6	–	7.6	–	70.3	–
Anterior <i>br</i> ratio	9	61.3	–	99.1				81.9		12.1			
Anterior total	12	13.5	–	17.9	37.1	–	45.3	15.5	41.1	1.6	2.7	15.1	44.8
Posterior base	16	0.4	–	14.6	1.1	–	36.1	10.3	27.8	3.1	7.7	10.2	30.0
Posterior primary branch	19	13.3	–	22.2	44.0	–	56.9	18.5	50.3	2.5	3.7	17.2	50.8
Posterior secondary branch	12	6.5	–	10.6	19.7	–	27.9	9.0	23.9	1.3	2.8	8.1	24.1
Posterior <i>cbt</i> ratio	15	47.7	–	70.2		–		58.7	–	6.6	–	59.0	–
Posterior <i>br</i> ratio	11	41.8	–	56.9				48.1		5.1			
Posterior total	14	24.2	–	37.3	72.6	–	92.1	29.4	79.1	4.3	5.9	24.9	73.5

Table 5 Summary of eggs morphometrics of *Ramazzottius claudii* sp. nov.

Character	N	Range		Mean		SD
Egg bare diameter	18	55.4	–	65.7	61.2	2.6
Egg full diameter	18	70.7	–	80.7	75.2	2.8
Process height	54	4.6	–	27.9	7.7	3.3
Process base width	54	0.6	–	2.9	1.3	0.4
Process base/height ratio	54	3%	–	43%	19%	7%
Inter-process distance	54	1.0	–	6.1	2.8	1.0
Number of processes on the egg circumference	12	40	–	52	46.3	3.5

- *Ramazzottius anomalus* (Ramazzotti, 1962): by having a thinner buccal tube [external diameter pt 11.5 in *R. anomalus* vs. 7.1 – 9.8 μm in *R. claudii* sp. nov.] and by the shape of the egg processes [long cone/aculeus in *R. anomalus* spines/filaments in *R. claudii* sp. nov.].
- *Ramazzottius groenlandensis* Kihm et al., 2023: by having smaller eggs [bare diameter 80.6 μm in *R. groenlandensis* vs. 55.4 – 65.7 μm in *R. claudii* sp. nov.] and by the processes shape [mostly cone shaped in *R. groenlandensis* vs. elongated spikes and filamentous in *R. claudii* sp. nov.].
- *Ramazzottius horningi* Binda & Pilato, 1994: by having longer external I–III claws [52.26 – 55.73 pt in *R. horningi* vs. 58.3 – 85.8 pt in *R. claudii* sp. nov.], and by the absence of a crown of dots around the base of the egg processes [crown of dots presents in *R. horningi* vs. absent in *R. claudii* sp. nov.].
- *Ramazzottius theroni* Dastych, 1993: by the absence of eyes [eyes present in *R. theroni* vs. absent in *R. claudii* sp. nov.] and a weakly visible cuticle sculpturing [very evident in *R. theroni* vs. weakly visible in *R. claudii* sp. nov.].
- *Ramazzottius valaamis* Biserov & Tumanov, 1993: by the shape of the egg processes [very thin filaments in *R. valaamis* vs. spines/filaments in *R. claudii* sp. nov.].

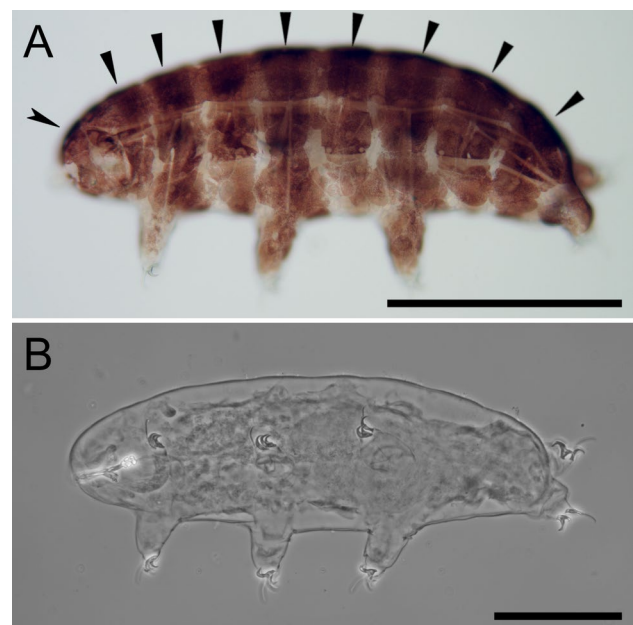
**Fig. 3** *Ramazzottius claudii* sp. nov. in toto. **A** In vivo animal under transmitted light showing pigmentation bands. **B** Holotype under PCM. Indented arrowheads: dorso-lateral pigmentation bands. Indented arrowhead: pigmentation ring around the mouth. Scale bars 100 μm

Fig. 4 *Ramazzottius claudii* sp. nov. cuticle under PCM. **A** Anterior dorsal cuticle. **B** Median dorsal cuticle. **C** Caudal dorsal cuticle. **D** Anterior dorsal cuticle in cross section. **E** Median dorsal cuticle in cross section. **F** Caudal dorsal cuticle in cross section. **G** Cuticle of a large individual showing “spindle” shaped granulation, more pronounced on the caudal side (on the right side of the image). White arrowhead: spindle-shaped granulation. Scale bars 20 μ m

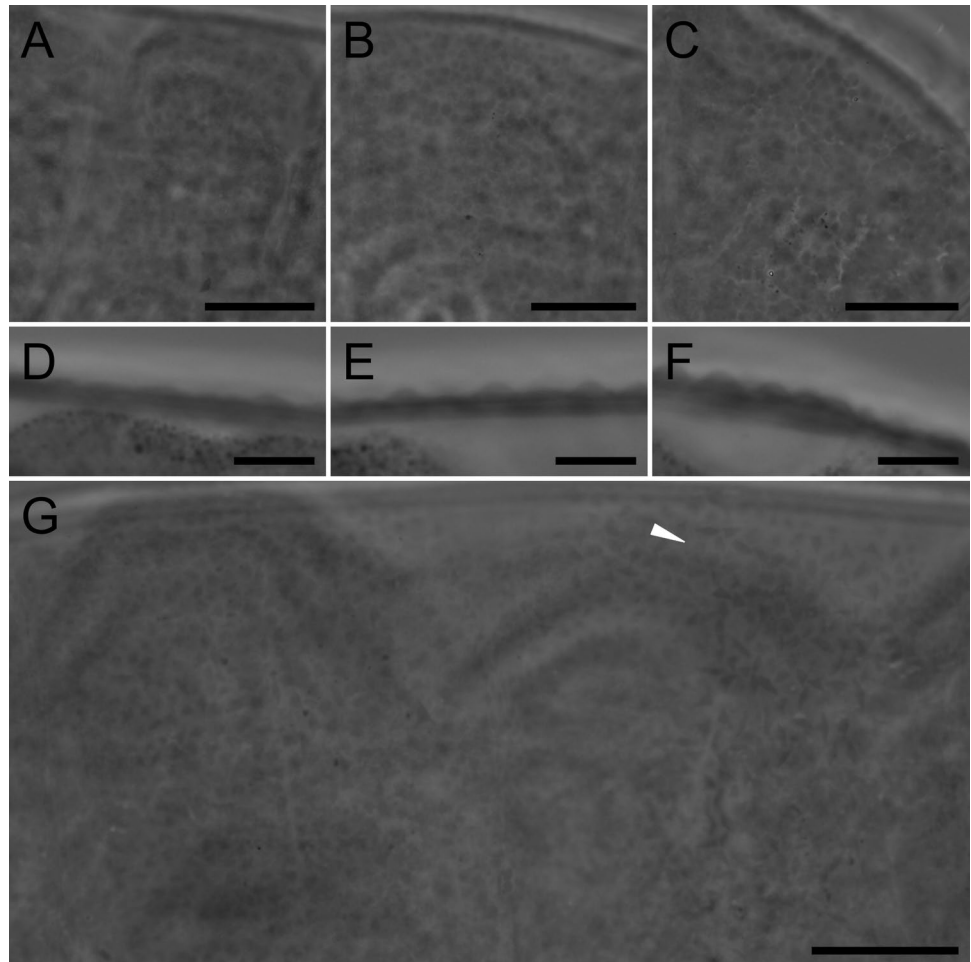


Fig. 5 *Ramazzottius claudii* sp. nov. cuticle under SEM. **A** Dorsal cephalic region showing sensory organs. **B** Dorsal caudal cuticle showing granular sculpture. **C** Dorsal caudal cuticle showing “spindle” like granulation. Arrowheads: cephalic sensory organs. White arrowhead: spindle-shaped granulation. Scale bars **A**, **C** 10 μ m; **B** 2 μ m

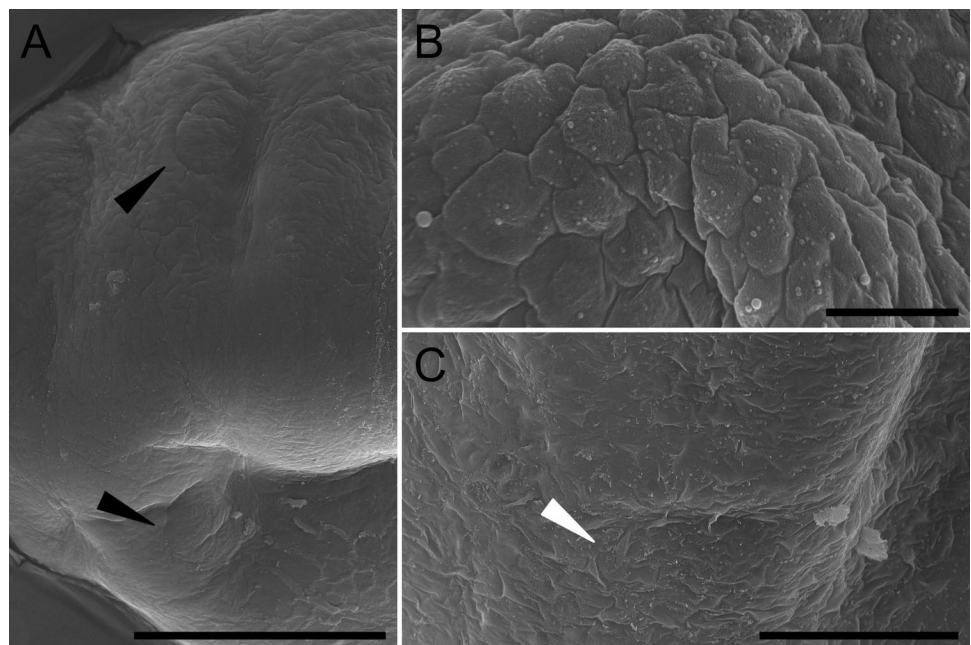
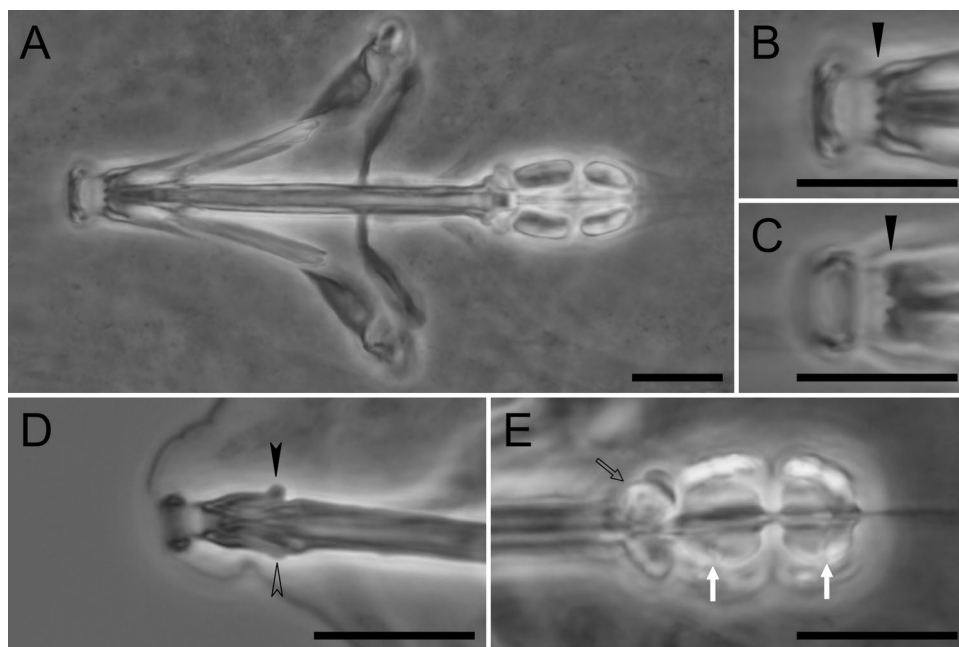


Fig. 6 *Ramazottius claudii* sp. nov. buccal apparatus under PCM. **A** Buccal apparatus *in toto* in dorsal view. **B** OCA in dorsal view. **C** Oral cavity armature (OCA) in ventral view. **D** AISM in lateral view. **E** Placoids in ventral view. Arrowheads: third band of OCA. Indented arrowhead: dorsal hook of AISM. Empty indented arrowhead: ventral hook of AISM. Empty arrow: pharyngeal apophyses. White arrows: macroplacoids constrictions. Scale bars 10 μ m

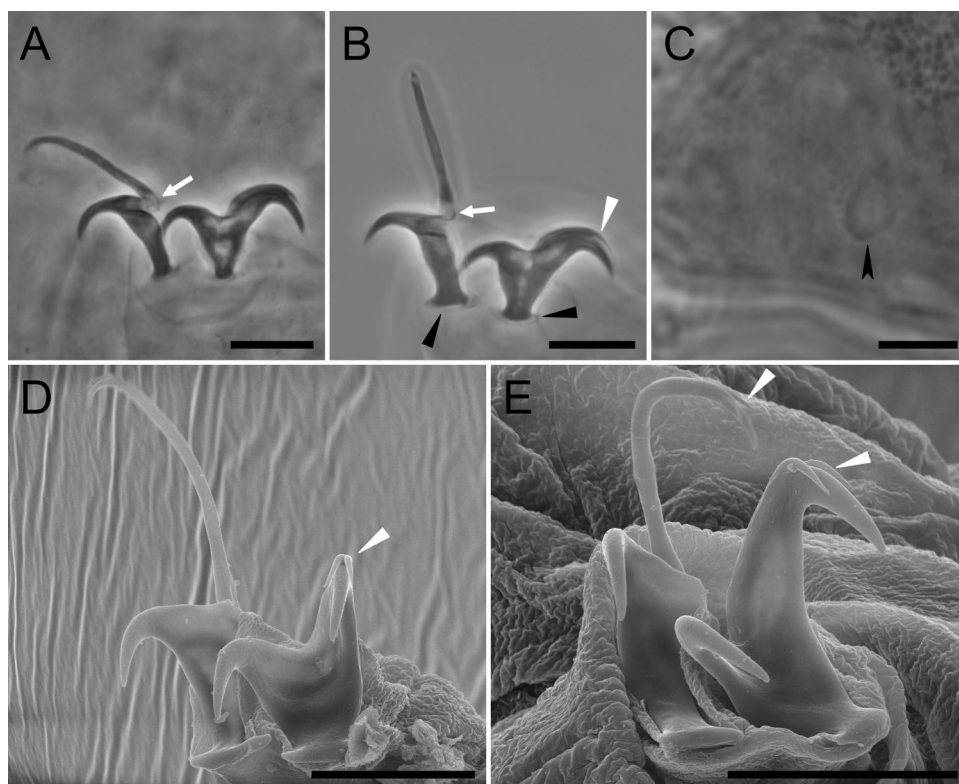


- *Ramazottius varieornatus* Bertolani & Kinchin, 1993: by having smaller eggs [bare diameter 69.9 – 73.3 μ m in *R. varieornatus* vs. 55.4 – 65.7 μ m in *R. claudii* sp. nov.], with generally longer processes [up to 10.2 μ m in *R. varieornatus* vs. up to 27.9 μ m in *R. claudii* sp. nov.], a shorter external claws II-III [58.2 – 68.6 *pt* in *R. varieornatus*

vs. 61.8 – 85.8 *pt* in *R. claudii* sp. nov.], and by the absence of males [absent in *R. varieornatus* vs. present in *R. claudii* sp. nov.].

Additionally, for five other *Ramazottius* species, the eggs are unknown; however, the new species differs from them by:

Fig. 7 *Ramazottius claudii* sp. nov. legs associated structures. **A** Claws III under PCM. **B** Claws IV under PCM. **C** Papilla on leg IV under PCM. **D** Claws III under SEM. **E** Claws IV under SEM. Black arrowheads: pseudolunules. White arrowheads: claws accessory points. White arrows: LRU with cuticular filaments. Indented arrowhead: Papilla on leg IV. Scale bars 10 μ m



- *Ramazzottius belubellus* Bartels et al., 2011: by the absence of spines on the dorsal cuticle [present in *R. belubellus* vs. absent in *R. claudii* sp. nov.].
- *Ramazzottius baumanni* (Ramazzotti, 1962): by the absence of stronged sculptured cuticle with elevated polygons [present in *R. baumanni* vs. absent in *R. claudii* sp. nov.].
- *Ramazzottius montivagus* (Dastych, 1983): by having a sculptured cuticle [smooth in *R. montivagus* vs. sculptured in *R. claudii* sp. nov.] and by more slender primary branch of external claws (morphometric data for *R. montivagus* not available, but see Figs. 5, 6, and 7 in Dastych, 1983).
- *Ramazzottius saltensis* (Claps & Rossi, 1984): by the absence of stronged sculptured cuticle with elevated polygons [present in *R. saltensis* vs. absent in *R. claudii* sp. nov.].
- *Ramazzottius szeptyckii* (Dastych, 1980): by the absence of dorsolateral gibbosities [present in *R. szeptycki* vs. absent in *R. claudii* sp. nov.].

Discussion

Despite being charismatic organisms, tardigrade biodiversity is still unexplored. In particular, some habitats have historically received less attention, and rock pools is one of them. Recently, tardigrades have been found and described from rock pools (Troell & Jönsson, 2023; Vecchi et al., 2022, 2023a, 2023b), showing the potential of this habitat for identifying a novel component of tardigrade diversity. Tardigrades from rock pools (and in particular the newly described *Ramazzottius*) are adapted to their extremely harsh conditions (multiple desiccation and freezing cycles) and show higher performances in surviving freeze–thaw cycles respect to congeneric taxa from other habitats (Zawierucha et al., 2023). The identification and description of this new tardigrade species with extreme resistance capabilities will be useful in finding new model taxa for the study of the molecular processes behind their incredible capabilities.

While one *Ramazzottius* species (*R. varieornatus* YOKOZUNA-1) recently became a popular model organism for

Fig. 8 *Ramazzottius claudii* sp. nov. eggs. **A–H** Eggs under PCM. **I** Egg under SEM. Scale bars 20 μ m

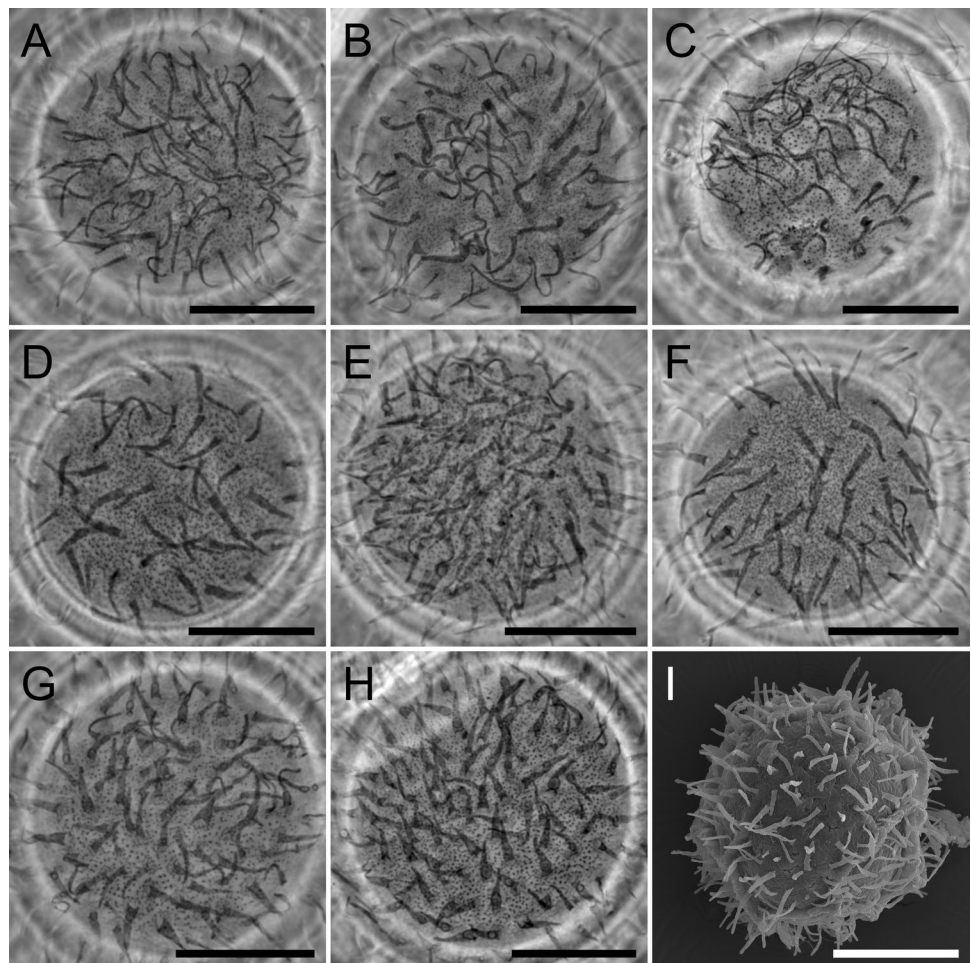
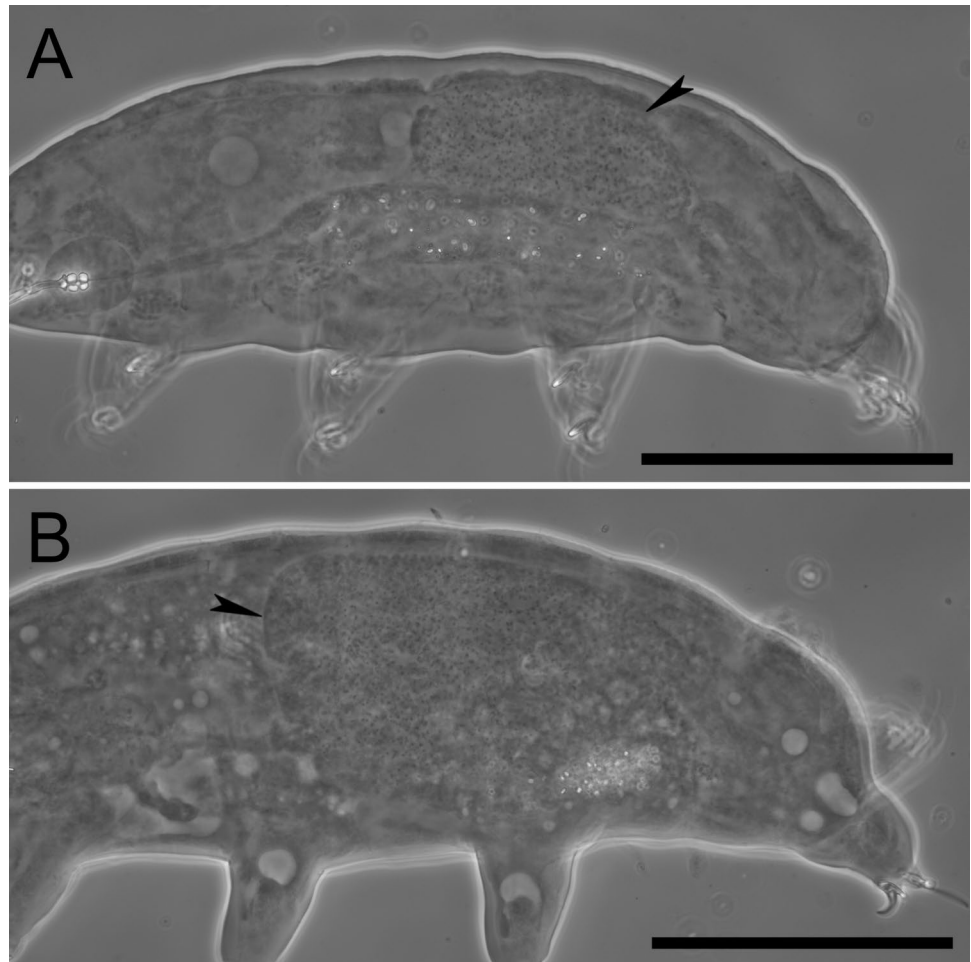


Fig. 9 *Ramazzottius claudii* sp. nov. males under PCM. **A–B** Males posterior part. Arrow-heads: gonads with developing spermatids. Scale bars 100 μ m



the study of the molecular mechanisms of stress resistance in tardigrades (e.g., Emdee et al., 2024; Horikawa et al., 2008, 2013; Neves et al., 2020), a comparative approach with multiple species would provide a more detailed knowledge of their molecular repertoire and evolution (Fleming et al., 2024). The newly described species is closely related to *R. varieornatus* YOKOZUNA-1 (Fig. 1), however they differ by their reproductive mode (parthenogenesis in *R. varieornatus* YOKOZUNA-1; Bertolani & Kinchin, 1993; Horikawa et al., 2008 vs. gonochorism in *R. claudii* sp. nov.) and probably by their cryptobiotic performances (*R. varieornatus* YOKOZUNA-1 was collected from a moss sample in Sapporo (Japan) at sea level, whereas the new species was collected in a shallow rock pool at ~1600 m a.s.l.; thus, they experience and are probably adapted to a different amount of environmental stress). Some anhydrobiosis related genes have been found to be differently expressed in the sexes in *Paramacrobiotus metropolitanus* Sugiura, Matsumoto & Kunieda, 2022 (Sugiura et al., 2024), and a similar phenomenon could occur in *Ramazzottius* too. Given its characteristic, the new species could be a potential candidate to

complement *R. varieornatus* YOKOZUNA-1 as model for the study of the molecular mechanisms behind cryptobiosis.

As the first step to provide resources on this new species, we sequenced its mitogenome and annotated its TDRPs (Temperature and Desiccation Resistance Proteins) genes. As expected, due to their phylogenetic proximity (Fig. 1), *R. claudii* sp. nov. and *R. varieornatus* YOKOZUNA-1 show a perfect synteny of their mitochondrial genes. However, the two genomes show a discrete nucleotidic divergence, in particular in the regions of the ATP synthase and nad2 genes (Fig. 2) which can reach a divergence higher than 30%. In context, the divergence in the cox1 gene (traditionally used in species delimitation and population genetic studies) in the two species examined here is about 17%. This suggests that another region of the mitochondrial genome could provide a more fine-scaled signal, which could be exploited in tardigrade species delimitation of closely related species and population genetics.

In addition to the mitogenome sequence, we identified TDRPs genes studied by Fleming et al. (2024) in different tardigrade taxa. Our results are congruent with what

found by Fleming et al. (2024) for *R. varieornatus* YOKOZUNA-1, with most of the TDRPs found in *R. claudii* sp. nov. In particular, the 15 identified CAHS genes show a close correspondence with the CAHS of *R. varieornatus* YOKOZUNA-1 (Table 2, Online resources 06) (Fleming et al., 2024), with the exception of CAHS6c that was not found in the new species. A less congruent situation was found for SAHS, where in the new species the SASH 9, 10, 11, and 13 were not identified and for one it was not possible to determine its homology with SAHS7 or 12 (Table 2, Online resources 06). Additionally, for the single copy of the MRE11 found in the new species, it was not possible to determine its homology to any of the 4 MRE11 identified in *R. varieornatus* YOKOZUNA-1, which form a monophyletic clade (Online resources 09) in sister group with the new *R. claudii* sp. nov. MRE11. This situation could suggest a possible expansion of the MRE11 genes in *R. varieornatus* YOKOZUNA-1; however, a more in-depth sequencing of the new species is required to confirm this hypothesis. Lastly, coherently to what was found in *R. varieornatus* YOKOZUNA-1, a single Dsup gene was also identified. Nevertheless, we showed that the TDRPs repertoire is conserved across closely related species even with contrasting reproductive modes and that the genome sequencing protocol used in this study is a viable solution for this task.

In conclusion, we described a new *Ramazzottius* species and provided novel genetic resources for the study of cryptobiosis molecular mechanisms.

Supplementary Information The online version contains supplementary material available at <https://doi.org/10.1007/s13127-024-00662-x>.

Acknowledgements This study was founded by the Polonez Bis grant No. 2022/45/P/NZ8/01512 to MV co-funded by the National Science Centre and the European Union framework Programme for Research and Innovation Horizon 2020 under the Marie Skłodowska-Curie grant agreement [No. 945339]. We wish to thank Dott. Izabela Potocka and Yelyzaveta Matsko (University of Silesia, Katowice, Poland) for help with the SEM stubs coating, and Dott. Claudio Ferrari (University of Parma, Italy) for his assistance during sampling.

Data availability The datasets generated during and analysed during the current study are available in the GenBank repository (see main text for accession numbers) or included in this published article [and its supplementary information files].

Declarations

Competing interests The authors declare no competing interests.

Open Access This article is licensed under a Creative Commons Attribution 4.0 International License, which permits use, sharing, adaptation, distribution and reproduction in any medium or format, as long as you give appropriate credit to the original author(s) and the source, provide a link to the Creative Commons licence, and indicate if changes were made. The images or other third party material in this article are included in the article's Creative Commons licence, unless indicated otherwise in a credit line to the material. If material is not included in

the article's Creative Commons licence and your intended use is not permitted by statutory regulation or exceeds the permitted use, you will need to obtain permission directly from the copyright holder. To view a copy of this licence, visit <http://creativecommons.org/licenses/by/4.0/>.

References

- Bartels, P. J., Nelson, D. R., Kaczmarek, Ł., & Michalczyk, Ł. (2011). *Ramazzottius belubellus*, a new species of Tardigrada (Eutardigrada: Parachela: Hypsibiidae) from the Great Smoky Mountains National Park (North Carolina, U.S.A.). *Proceedings of the Biological Society of Washington*, 124(1), 23–27. <https://doi.org/10.2988/10-13.1>
- Bernt, M., Donath, A., Jühling, F., Externbrink, F., Florentz, C., Fritzsche, G., Pütz, J., Middendorf, M., & Stadler, P. F. (2013). MITOS: Improved de novo metazoan mitochondrial genome annotation. *Molecular Phylogenetics and Evolution*, 69(2), 313–319. <https://doi.org/10.1016/j.ympev.2012.08.023>
- Bertolani, R., & Kinchin, I. M. (1993). A new species of *Ramazzottius* (Tardigrada, Hypsibiidae) in a rain gutter sediment from England. *Zoological Journal of the Linnean Society*, 109(3), 327–333. <https://doi.org/10.1111/j.1096-3642.1993.tb02538.x>
- Binda, M. G., & Pilato, G. (1986). *Ramazzottius*, nuovo genere di Eutardigrada (Hypsibiidae). *Animalia*, 13, 159–166.
- Binda, M., & Pilato, G. (1994). Notizie sui Tardigradi delle Isole Hawaii con descrizione di due specie nuove. *Animalia*, 21(1/3), 57–62.
- Biserov, V. (1997). Tardigrades of the Caucasus with a taxonomic analysis of the genus *Ramazzottius* (Parachela: Hypsibiidae). *Zoologischer Anzeiger*, 236, 139–159.
- Biserov, V., & Tumanov, D. (1993). *Ramazzottius valaamii* sp. n. (Tardigrada, Gypsibiidae), a new species of tardigrads from Valaam Island, Karelia, Russia. *Zoologičeskij Žurnal*, 72(11), 35–39.
- Buchfink, B., Xie, C., & Huson, D. H. (2015). Fast and sensitive protein alignment using DIAMOND. *Nature Methods*, 12(1), 59–60. <https://doi.org/10.1038/nmeth.3176>
- Camarda, D., Massa, E., Guidetti, R., & Lisi, O. (2023). A new, simplified, drying protocol to prepare tardigrades for scanning electron microscopy. *Microscopy Research and Technique*, jemt.24460. <https://doi.org/10.1002/jemt.24460>
- Casquet, J., Thebaud, C., & Gillespie, R. G. (2012). Chelex without boiling, a rapid and easy technique to obtain stable amplifiable DNA from small amounts of ethanol-stored spiders. *Molecular Ecology Resources*, 12(1), Article 1. <https://doi.org/10.1111/j.1755-0998.2011.03073.x>
- Claps, M. C., & Rossi, G. C. (1984). Contribución al conocimiento de los tardígrados de Argentina. IV. *Acta Zoologica Lilloana*, 38(1), 45–50.
- Dastych, H. (1980). *Hypsibius szeptycki* sp. nov., a new species of Tardigrada from South Africa. *Bull Bulletin de L'Academie Polonaise des Sciences Série des Sciences Biologiques*, 26(6), 505–508.
- Dastych, H. (1983). Two new eutardigrada species from West Spitsbergen and the Tatra mts. *Bulletin De La Société Des Amis Des Sciences Et Des Lettres De Poznan*, 23, 195–200.
- Dastych, H. (1993). A new genus and four new species of semiterrestrial water-bears from South Africa (Tardigrada). *Mitteilungen Aus Dem Naturhistorischen Museum in Hamburg*, 90, 175–186.
- De Coster, W., & Rademakers, R. (2023). NanoPack2: Population-scale evaluation of long-read sequencing data. *Bioinformatics*, 39(5), btad311. <https://doi.org/10.1093/bioinformatics/btad311>
- Dey, P. K., López-López, A., Morek, W., & Michalczyk, Ł. (2024). Tardigrade Augean stables—A challenging phylogeny and taxonomy

- of the family Ramazzottiidae (Eutardigrada: Hypsibiidae). *Zoological Journal of the Linnean Society*, 200(1), 95–110. <https://doi.org/10.1093/zoolinnean/zlad161>
- Donath, A., Jühling, F., Al-Arab, M., Bernhart, S. H., Reinhardt, F., Stadler, P. F., Middendorf, M., & Bernt, M. (2019). Improved annotation of protein-coding genes boundaries in metazoan mitochondrial genomes. *Nucleic Acids Research*, 47(20), 10543–10552. <https://doi.org/10.1093/nar/gkz833>
- Edgar, R. C. (2004). MUSCLE: Multiple sequence alignment with high accuracy and high throughput. *Nucleic Acids Research*, 32(5), 1792–1797. <https://doi.org/10.1093/nar/gkh340>
- Emdee, N., Møbjerg, A., Grollmann, M. M., & Møbjerg, N. (2024). Osmotic stress tolerance and transcriptomic response of *Ramazzottius varieornatus* (Eutardigrada: Ramazzottiidae) following tun formation. *Zoological Journal of the Linnean Society*, 200(1), 220–229. <https://doi.org/10.1093/zoolinnean/zlad046>
- Faurby, S., Jönsson, K. I., Rebecchi, L., & Funch, P. (2008). Variation in anhydrobiotic survival of two eutardigrade morphospecies: A story of cryptic species and their dispersal. *Journal of Zoology*, 275(2), Article 2. <https://doi.org/10.1111/j.1469-7998.2008.00420.x>
- Fleming, J. F., Pisani, D., & Arakawa, K. (2024). The evolution of temperature and desiccation-related protein families in Tardigrada reveals a complex acquisition of extremotolerance. *Genome Biology and Evolution*, 16(1), evad217. <https://doi.org/10.1093/gbe/evad217>
- GIMP Development Team. (2019). *GIMP*. <https://www.gimp.org>
- Greiner, S., Lehwark, P., & Bock, R. (2019). OrganellarGenomeDRAW (OGDRAW) version 1.3.1: Expanded toolkit for the graphical visualization of organellar genomes. *Nucleic Acids Research*, 47(W1), W59–W64. <https://doi.org/10.1093/nar/gkz238>
- Guidetti, R., Cesari, M., Giovannini, I., Ebel, C., Förschler, M. I., Rebecchi, L., & Schill, R. O. (2022). Morphology and taxonomy of the genus *Ramazzottius* (Eutardigrada: Ramazzottiidae) with the integrative description of *Ramazzottius kretschmanni* sp. nov. *European Zoological Journal*, 89(1), 346–370. <https://doi.org/10.1080/24750263.2022.2043468>
- Guidetti, R., Massa, E., Bertolani, R., Rebecchi, L., & Cesari, M. (2019). Increasing knowledge of Antarctic biodiversity: New endemic taxa of tardigrades (Eutardigrada: Ramazzottiidae) and their evolutionary relationships. *Systematics and Biodiversity*, 17(6), 573–593. <https://doi.org/10.1080/14772000.2019.1649737>
- Guil, N., & Giribet, G. (2012). A comprehensive molecular phylogeny of tardigrades—adding genes and taxa to a poorly resolved phylum-level phylogeny. *Cladistics*, 28(1), 21–49. <https://doi.org/10.1111/j.1096-0031.2011.00364.x>
- Guy, L., Roat Kultima, J., & Andersson, S. G. E. (2010). genoPlotR: Comparative gene and genome visualization in R. *Bioinformatics (Oxford, England)*, 26(18), 2334–2335. <https://doi.org/10.1093/bioinformatics/btq413>
- Hashimoto, T., Horikawa, D. D., Saito, Y., Kuwahara, H., Kozuka-Hata, H., Shin-i, T., et al. (2016). Extremotolerant tardigrade genome and improved radiotolerance of human cultured cells by tardigrade-unique protein. *Nature Communications*, 7(1), 12808. <https://doi.org/10.1038/ncomms12808>
- Hengherr, S., & Schill, R. O. (2018). Environmental adaptations: Cryobiosis. In Schill, R. (Eds), *Water bears: The biology of Tardigrades*. (Vol. 2, pp. 295–310). Springer. https://doi.org/10.1007/978-3-319-95702-9_11
- Hoff, K. J., & Stanke, M. (2013). WebAUGUSTUS—A web service for training AUGUSTUS and predicting genes in eukaryotes. *Nucleic Acids Research*, 41(W1), 123–128. <https://doi.org/10.1093/nar/gkt418>
- Horikawa, D. D. (2008). The Tardigrade *Ramazzottius varieornatus* as a model animal for astrobiological studies. *Biological Sciences in Space*, 22(3), 93–98. <https://doi.org/10.2187/bss.22.93>
- Horikawa, D. D., Cumbers, J., Sakakibara, I., Rogoff, D., Leuko, S., Harnoto, R., Arakawa, K., Katayama, T., Kunieda, T., Toyoda, A., Fujiyama, A., & Rothschild, L. J. (2013). Analysis of DNA repair and protection in the Tardigrade *Ramazzottius varieornatus* and *Hypsibius dujardini* after exposure to UVC radiation. *PLoS ONE*, 8(6), Article 6. <https://doi.org/10.1371/journal.pone.0064793>
- Horikawa, D. D., Kunieda, T., Abe, W., Watanabe, M., Nakahara, Y., Yukuhiro, F., Sakashita, T., Hamada, N., Wada, S., Funayama, T., Katagiri, C., Kobayashi, Y., Higashi, S., & Okuda, T. (2008). Establishment of a rearing system of the extremotolerant tardigrade *Ramazzottius varieornatus*: A new model animal for astrobiology. *Astrobiology*, 8(3), 549–556. <https://doi.org/10.1089/ast.2007.0139>
- Inkscape Project. (2020). *Inkscape*. <https://inkscape.org>
- Katoh, K. (2002). MAFFT: A novel method for rapid multiple sequence alignment based on fast Fourier transform. *Nucleic Acids Research*, 30(14), Article 14. <https://doi.org/10.1093/nar/gkf436>
- Katoh, K., & Toh, H. (2008). Recent developments in the MAFFT multiple sequence alignment program. *Briefings in Bioinformatics*, 9(4), Article 4. <https://doi.org/10.1093/bib/bbn013>
- Kihm, J.-H., Zawierucha, K., Rho, H. S., & Park, T.-Y.S. (2023). Homology of the head sensory structures between Heterotardigrada and Eutardigrada supported in a new species of water bear (Ramazzottiidae: Ramazzottiidae). *Zoological Letters*, 9(1), 22. <https://doi.org/10.1186/s40851-023-00221-w>
- Kolmogorov, M., Yuan, J., Lin, Y., & Pevzner, P. A. (2019). Assembly of long, error-prone reads using repeat graphs. *Nature Biotechnology*, 37(5), 540–546. <https://doi.org/10.1038/s41587-019-0072-8>
- Lanfear, R., Frandsen, P. B., Wright, A. M., Senfeld, T., & Calcott, B. (2016). PartitionFinder 2: New methods for selecting partitioned models of evolution for molecular and morphological phylogenetic analyses. *Molecular Biology and Evolution*, msw260. <https://doi.org/10.1093/molbev/msw260>
- Lin, Y., Yuan, J., Kolmogorov, M., Shen, M. W., Chaisson, M., & Pevzner, P. A. (2016). Assembly of long error-prone reads using de Bruijn graphs. *Proceedings of the National Academy of Sciences*, 113(52), E8396–E8405. <https://doi.org/10.1073/pnas.1604560113>
- Michalczyk, Ł., & Kaczmarek, Ł. (2013). The Tardigrada Register: A comprehensive online data repository for tardigrade taxonomy. *Journal of Limnology*, 72(s1), 175–181. <https://doi.org/10.4081/jlimnol.2013.s1.e22>
- Møbjerg, N., Jørgensen, A., Eibye-Jacobsen, J., Agerlin Halberg, K., Persson, D. K., & Møbjerg Kristensen, R. (2007). New records on cyclomorphosis in the marine eutardigrade *Halobiotus crispae* (Eutardigrada: Hypsibiidae). *Journal of Limnology*, 66(s 1), 132–140. <https://doi.org/10.4081/jlimnol.2007.s1.132>
- Mutterer, J., & Zinck, E. (2013). Quick-and-clean article figures with FigureJ. *Journal of Microscopy*, 252(1), 89–91. <https://doi.org/10.1111/jmi.12069>
- Nelson, D. R., Bartels, P. J., & Guil, N. (2018). Tardigrade ecology. In Schill, R. (Eds), *Water Bears: The Biology of Tardigrades*. (Vol. 2, pp. 163–210). Springer. https://doi.org/10.1007/978-3-319-95702-9_7
- Neves, R. C., Hvidepil, L. K. B., Sørensen-Hygum, T. L., Stuart, R. M., & Møbjerg, N. (2020). Thermotolerance experiments on active and desiccated states of *Ramazzottius varieornatus* emphasize that tardigrades are sensitive to high temperatures. *Scientific Reports*, 10(1), Article 94. <https://doi.org/10.1038/s41598-019-56965-z>
- Nishimura, O., Hara, Y., & Kuraku, S. (2017). gVolante for standardizing completeness assessment of genome and transcriptome assemblies. *Bioinformatics*, 33(22), 3635–3637. <https://doi.org/10.1093/bioinformatics/btx445>

- Pedersen, T. L. (2023). *patchwork: The composer of plots*. <https://CRAN.R-project.org/package=patchwork>. Accessed 10 June 2024.
- Pilato, G. (1981). Analisi di nuovi caratteri nello studio degli Eutardigradi. *Animalia*, 8, 51–57.
- Ramazzotti, G. (1962). Tardigradi del Cile, con descrizione di quattro nuove specie di una nuova varietà. *Atti Della Società Italiana Di Scienze Naturali e Del Museo Civico Di Storia Naturale in Milano*, 101, 275–287.
- Rambaut, A. (2007). *FigTree, a graphical viewer of phylogenetic trees*. <http://tree.bio.ed.ac.uk/software/figtree/>. Accessed 10 June 2024.
- Rambaut, A., Drummond, A. J., Xie, D., Baele, G., & Suchard, M. A. (2018). Posterior summarization in Bayesian phylogenetics using Tracer 1.7. *Systematic Biology*, 67(5), Article 5. <https://doi.org/10.1093/sysbio/syy032>
- Rebecchi, L., Altiero, T., & Guidetti, R. (2007). Anhydrobiosis: The extreme limit of desiccation tolerance. *Invertebrate Survival Journal*, 4(2), 65–81.
- Ronquist, F., Teslenko, M., van der Mark, P., Ayres, D. L., Darling, A., Höhna, S., Larget, B., Liu, L., Suchard, M. A., & Huelsenbeck, J. P. (2012). MrBayes 3.2: Efficient Bayesian phylogenetic inference and model choice across a large model space. *Systematic Biology*, 61(3), Article 3. <https://doi.org/10.1093/sysbio/sys029>
- Schill, R. O. (Ed.). (2018). *Water bears: The biology of Tardigrades* (Vol. 2). Springer. <https://doi.org/10.1007/978-3-319-95702-9>
- Schill, R. O., & Hengherr, S. (2018). Environmental adaptations: Desiccation tolerance. In Schill, R. (Eds), *Water Bears: The Biology of Tardigrades*. (pp. 273–293). Springer. https://doi.org/10.1007/978-3-319-95702-9_10
- Simão, F. A., Waterhouse, R. M., Ioannidis, P., Kriventseva, E. V., & Zdobnov, E. M. (2015). BUSCO: Assessing genome assembly and annotation completeness with single-copy orthologs. *Bioinformatics*, 31(19), 3210–3212. <https://doi.org/10.1093/bioinformatics/btv351>
- Stanke, M., Diekhans, M., Baertsch, R., & Haussler, D. (2008). Using native and syntenically mapped cDNA alignments to improve *de novo* gene finding. *Bioinformatics*, 24(5), 637–644. <https://doi.org/10.1093/bioinformatics/btn013>
- Stec, D., Kristensen, R. M., & Michalczyk, Ł. (2020). An integrative description of *Minibiotus ioculator* sp. nov. from the Republic of South Africa with notes on *Minibiotus pentannulatus* Londoño et al., 2017 (Tardigrada: Macrobiotidae). *Zoologischer Anzeiger*, 286, 117–134. <https://doi.org/10.1016/j.jcz.2020.03.007>
- Stec, D., Morek, W., Gasiorek, P., Kaczmarek, Ł., & Michalczyk, Ł. (2016). Determinants and taxonomic consequences of extreme egg shell variability in *Ramazzottius subanomalus* (Biserov, 1985) (Tardigrada). *Zootaxa*, 4208(2), 176–188. <https://doi.org/10.11646/zootaxa.4208.2.5>
- Stec, D., Morek, W., Gasiorek, P., & Michalczyk, Ł. (2018). Unmasking hidden species diversity within the *Ramazzottius oberhaeuseri* complex, with an integrative redescription of the nominal species for the family Ramazzottiidae (Tardigrada: Eutardigrada: Parachela). *Systematics and Biodiversity*, 16(4), 357–376. <https://doi.org/10.1080/14772000.2018.1424267>
- Stec, D., Zawierucha, K., & Michalczyk, Ł. (2017). An integrative description of *Ramazzottius subanomalus* (Biserov, 1985) (Tardigrada) from Poland. *Zootaxa*, 4300(3), 403–420. <https://doi.org/10.11646/zootaxa.4300.3.4>
- Sugiura, K., Yoshida, Y., Hayashi, K., Arakawa, K., Kunieda, T., & Matsumoto, M. (2024). Sexual dimorphism in the tardigrade *Paramacrobiotus metropolitanus* transcriptome. *Zoological Letters*, 10(1), 11. <https://doi.org/10.1186/s40851-024-00233-0>
- Thulin, G. (1911). Beiträge zur kenntnis der tardigradenfauna schwedens. *Arkiv För Zoology*, 7, 1–60.
- Trifinopoulos, J., Nguyen, L. T., von Haeseler, A., & Minh, B. Q. (2016). W-IQ-TREE: A fast online phylogenetic tool for maximum likelihood analysis. *Nucleic Acids Research*, 44(1), 232–235. <https://doi.org/10.1093/nar/gkw256>
- Troell, S., & Jönsson, K. I. (2023). Occurrence of tardigrades and morphometric and chemical conditions in rock pools by the Baltic Sea. *Scientific Reports*, 13(1), 19776. <https://doi.org/10.1038/s41598-023-46697-6>
- Vecchi, M., & Bruneaux, M. (2021). *concatipede: An R package to concatenate fasta sequences easily*. <https://doi.org/10.5281/zenodo.5130604>
- Vecchi, M., Ferrari, C., Stec, D., & Calhim, S. (2022). Desiccation risk favours prevalence and diversity of tardigrade communities and influences their trophic structure in alpine ephemeral rock pools. *Hydrobiologia*, 849(9), 1995–2007. <https://doi.org/10.1007/s10750-022-04820-0>
- Vecchi, M., McDaniel, J. L., Chartrain, J., Vuori, T., Walsh, E. J., & Calhim, S. (2023a). Morphology, phylogenetic position, and mating behaviour of a new *Mesobiotus* (Tardigrada) species from a rock pool in the Socorro Box Canyon (New Mexico, USA). *The European Zoological Journal*, 90(2), 708–725. <https://doi.org/10.1080/24750263.2023.2263033>
- Vecchi, M., Tsvetkova, A., Stec, D., Ferrari, C., Calhim, S., & Tumanov, D. (2023b). Expanding *Acutuncus*: Phylogenetics and morphological analyses reveal a considerably wider distribution for this tardigrade genus. *Molecular Phylogenetics and Evolution*, 180, 107707. <https://doi.org/10.1016/j.ympev.2023.107707>
- Wick, R. R., Schultz, M. B., Zobel, J., & Holt, K. E. (2015). Bandage: Interactive visualization of *de novo* genome assemblies. *Bioinformatics*, 31(20), 3350–3352. <https://doi.org/10.1093/bioinformatics/btv383>
- Wickham, H. (2016). *ggplot2: Elegant graphics for data analysis*. Springer-Verlag New York. <https://ggplot2.tidyverse.org>. Accessed 10 June 2024.
- Wilkins, D. (2024). *gggenes: Draw gene arrow maps in 'ggplot2'*. <https://wilcox.org/gggenes/>. Accessed 10 June 2024.
- Zawierucha, K., Ostrowska, M., Vonnahme, T. R., Devetter, M., Nawrot, A. P., Lehmann, S., & Kolicka, M. (2016). Diversity and distribution of Tardigrada in Arctic cryoconite holes. *Journal of Limnology*, 75(3), 545–559. <https://doi.org/10.4081/jlimnol.2016.1453>
- Zawierucha, K., Stec, D., Lachowska-Cierlik, D., Takeuchi, N., Li, Z., & Michalczyk, Ł. (2018). High Mitochondrial Diversity in a New Water Bear Species (Tardigrada: Eutardigrada) from Mountain Glaciers in Central Asia, with the Erection of a New Genus *Cryoconicus*. *Annales Zoologici*, 68(1), 179–201. <https://doi.org/10.3161/00034541anz2018.68.1.007>
- Zawierucha, K., Vecchi, M., Takeuchi, N., Ono, M., & Calhim, S. (2023). Negative impact of freeze–thaw cycles on the survival of tardigrades. *Ecological Indicators*, 154, 110460. <https://doi.org/10.1016/j.ecolind.2023.110460>
- Zeglinski, K., Hsu, A., Alhamdoosh, M., & Koutsakis, C. (2021). *gmoviz: Seamless visualization of complex genomic variations in GMOs and edited cell lines*. <https://github.com/malhamdoosh/gmoviz>. Accessed 10 June 2024.

Publisher's Note Springer Nature remains neutral with regard to jurisdictional claims in published maps and institutional affiliations.